







Open Archive Toulouse Archive Ouverte (OATAO)

OATAO is an open access repository that collects the work of Toulouse researchers and makes it freely available over the web where possible

This is an author's version published in: <http://oatao.univ-toulouse.fr/28410>

Official URL: <https://doi.org/10.1016/j.porgcoat.2021.106163>

To cite this version:

Bonin, Pierre  and Roggero, Aurélien  and Caussé, Nicolas  and Pébère, Nadine  and Thierry, Dominique and Le Bozec, Nathalie *Impedance analysis of the barrier effect of coil-coated materials: Water uptake and glass transition variations.* (2021) *Progress in Organic Coatings*, 153. 106163. ISSN 0300-9440

Any correspondence concerning this service should be sent to the repository administrator: tech-oatao@listes-diff.inp-toulouse.fr

Impedance analysis of the barrier effect of coil-coated materials: Water uptake and glass transition variations

Pierre Bonin^{a,b}, Aurélien Roggero^a, Nicolas Causse^{a,*}, Nadine Pébère^a, Dominique Thierry^b, Nathalie Le Bozec^b

^a Université de Toulouse, CERIMAT-ENSIACET, 4 allée Emile Monso, BP44362, 31030, Toulouse Cedex 4, France

^b Institut de la Corrosion / French Corrosion Institute, 220 rue Pierre Rivoalon, 29200, Brest, France

ARTICLE INFO

Keywords:

Coil coating
Electrochemical impedance spectroscopy
Water sorption
Barrier properties
Plasticization

ABSTRACT

In the present work, an industrial polyester coil-coated steel sample was characterized by electrochemical impedance spectroscopy. The diagrams were obtained for various immersion times in a 0.5 M NaCl solution for three different initial states of the same coil coating (as received, dried and dried after the impedance measurement). The aim of the study was to have a better knowledge of how the water uptake influences the coil coating physical properties and to extract relevant parameters of the ageing processes. From the high-frequency part of the impedance diagrams, the water uptake was calculated using a linear rule of mixtures. Two sorption regions were observed for the dried samples suggesting the presence of porosities already filled with ambient moisture for the as-received sample. It was shown that the water uptake was a slow process and, independently of the initial state of the sample, a saturation plateau was never reached, even after 456 h of immersion. A time constant, clearly visible on the phase angle of the impedance diagrams, was analysed through the dielectric permittivity formalism and attributed to the signature of the dielectric manifestation of the glass transition. This time constant was shifted to higher frequencies with increasing water fraction (increasing immersion time), consistent with a plasticization effect. This result was supported by differential scanning calorimetry measurements. Finally, the data obtained for the different initial states of the coating highlighted that, even if the water uptake was reversible, the sorption kinetics was different for the sample dried after the impedance measurements. This could be of importance in the degradation process of the coil coated steel.

1. Introduction

Coil coatings materials, used in the building industry, are able to protect the steel in outdoor environments for a long time but might be subject to different deterioration processes such as blistering, corrosion at cut-edges and early degradation of highly deformed regions [1,2]. The tendency of a paint system to blistering depends on several parameters, including surface contaminations, bulk properties of the polymer and interactions at the metal/polymer interface [3–5]. The environmental conditions, such as humidity and exposure to UV, also have an effect on blistering appearance [6,7]. Polymer adhesion to the metal substrate, and more particularly wet adhesion, is envisaged to have a primary role on the blistering appearance [4,8–11]. Water uptake is also considered to play an important role on the coating degradation. Water uptake can be determined from gravimetry or electrochemical impedance spectroscopy [12–15]. Infrared spectroscopy can also be used to analyse

water transport [16,17]. To calculate the water uptake from the high frequency part of the impedance diagrams, the Brasher and Kingsbury equation is often used [13] but this equation is known to overestimate water uptake values compared to gravimetric measurements [13, 18–21]. In various studies, a linear rule of mixture showed that the obtained values were consistent with those obtained from gravimetry [20–22]. One of the main advantages of using impedance data instead of gravimetry is the continuous monitoring of the water uptake without the need to remove the samples from the electrolytic solution.

Water penetration within a thermoset coating is a complex process which occurs at different scales [23,24]. The most frequently mentioned is the water penetration through preferential pathways, such as pores or low cross-linked areas of the polymer [24–28]. Water sorption into the polymer matrix is governed by interactions between water and some specific segments or groups in the polymer and by the available free volume [23,29,30]. These interactions modify the polymer's mobility (*i.*

* Corresponding author.

E-mail address: nicolas.causse@ensiacet.fr (N. Causse).

e. the glass transition [31–33]) over immersion time and more particularly its mechanical [34] and dielectric properties [35]. More than the amount of water intake in the polymer, the ability of a coating to completely desorb water rapidly and without significant changes seems to enhance its durability [36,37]. The water uptake within the coating can induce a plasticization of the polymer which can switch from the vitreous state to the rubbery state, changing water sorption mechanism, and allowing an increase in water content [19,32,38]. The glass transition is usually investigated through differential scanning calorimetry (DSC), dynamic mechanical analysis (DMA), or broadband dielectric spectroscopy (BDS) [32,39,40].

Moreover, different effects can be induced by water uptake on the coatings, such as swelling, water accumulation at the metal/polymer interface and mechanical stress in the coating [41–43]. These phenomena can provoke blistering through loss of adhesion and/or corrosion development [3,5,11,44]. The ionic transport within the polymer may also have an effect on its anti-corrosive performance. The kinetics of diffusion of oxygen and water within the coating are too fast to be the limiting factor in the appearance of corrosion [25,35,45]. Some authors assumed that the limiting factor should be the diffusion of ions to the metal/coating interface [25,35].

Electrochemical impedance spectroscopy (EIS) also allows several relevant parameters of the coating to be extracted over the whole duration of the experiments [15,46–48]. The barrier properties of the coating can be assessed through the low frequency impedance modulus. This value is often used to rank different organic coatings, the higher its value the better the barrier properties are supposed to be [25,37,46]. The impedance diagrams sometimes display modifications with increasing immersion time and appearance of new time constants, which could be linked to changes in the polymer properties. Some authors have discussed these time constants to be the manifestation of heterogeneities in water sorption within the coating (low cross-linked areas, for example) [45], and other authors, as the appearance of a swelling gradient [49]. More recently, the presence of a time constant associated with the dielectric manifestation of the glass transition (marker of the molecular mobility) has been shown from EIS data [21,39].

The aim of the present work is to have a better knowledge of the initial steps which control the degradation process of coil coated steel and more particularly, to analyse the influence of water ingress on the physical structure of the coil coating in order to identify relevant parameters of the ageing process. To achieve this goal, an industrial polyester coil coated steel was characterized by EIS. Three different initial states of the coil coating were considered. The impedance diagrams were obtained for various immersion times in a 0.5 M NaCl solution. An approach combining conventional impedance spectroscopy, dielectric spectroscopy (Cole-Cole analysis) and calorimetry (T_g measurement) was proposed.

2. Experimental

2.1. Coil coated sample

The commercial coil coating was composed of a galvanized steel (hot-dip galvanized steel with a zinc coating of 275 g/m²) on which a chromium-free primer and a topcoat were deposited. Both polymer layers were based on polyester (PES) chemistry with a thickness of 5 μ m and 20 μ m for the primer and the topcoat, respectively. The primer was a polyester/melamine/epoxy system with a total pigment volume concentration (PVC) of 18 %, containing phosphates as inhibitive pigments. The topcoat was a polyester/melamine system with a total PVC of 22 %. A surface treatment, based on Ti and Zr chemistry was applied before the primer deposition.

2.2. Electrochemical impedance spectroscopy

Impedance measurements were performed by using the Paint Cell

Test (from Gamry). The coil-coated sample constituted the working electrode while a graphite rod acted as both counter and reference electrodes (two electrode configuration). The advantage of this configuration is to measure impedance at high frequencies without artefacts linked to the use of a reference electrode. The measurements were carried out using a Gamry REF600 apparatus. The impedance diagrams were obtained every 2 h for 72 h and then, once a day for 16 days, for a total immersion time of 456 h (19 days), over a frequency range of 100 kHz to 0.01 Hz with 8 points per decade. An additional series of experiments was performed in a reduced frequency range (100 kHz to 1 Hz) every 90 s during the first 72 h. All the diagrams were obtained with a 20 mV_{rms} sinusoidal voltage perturbation at a potential of 0 V versus the reference electrode to avoid capacitive drift of the open circuit potential during the first hours of experiment [50]. The application of an arbitrary potential is possible here due to the absence of corrosion. The electrochemical cell was placed in a Faraday cage. The measurements were carried out in a 0.5 M NaCl solution at room temperature. The surface area of the coil coated material in contact with the electrolyte was 14.6 cm². The impedance results are shown for a single sample but they are typical of the studied coil coating. The margins of error were calculated from student's law on the standard deviation for three replicates and for a confidence interval of 95 %.

2.3. Exposure conditions

Three different states of the coil coating were studied through EIS measurements. The first series of experiments was conducted on the as-received sample, referred in the following as "as-received". The as-received coil coating was stored at room temperature under less than 50 % relative humidity over about one year. The second series of EIS measurements was performed to study the effect of an ageing process on the coating. The as-received sample was dried for 16 h at 60 °C (referred in the following as "Dry 1st imm."). Impedance diagrams were obtained on the dry sample during 19 days of immersion in the 0.5 M NaCl solution. Then, the experiment was stopped; the sample was removed from the exposure to the electrolytic solution and dried at 60 °C for 16 h. Then, EIS measurements were performed again for 19 days of immersion in the NaCl solution (referred in the following as "Dry 2nd imm.").

Different drying protocols were tested and thermogravimetric analysis (TGA) was performed on the as-received sample. No significant mass loss (below 1 %) was noticed during 16 h at 60 °C by the TGA measurements (results not shown). The temperature of 60 °C corresponds to the lowest temperature to avoid the influence of drying on the polymer structure and 16 h corresponds to a sufficient time to remove water.

2.4. Differential scanning calorimetry

DSC experiments were carried out with a TA Instruments Discovery DSC 250 apparatus under inert atmosphere (He). A heating ramp from -60 °C to 130 °C was performed at a heating rate of 20 °C/min. The coating was taken from a coil coated plate with a metallic tool, taking care to scrape both the primer and the top coat whilst avoiding metallic part of the galvanized steel substrate. The different initial states of the coil coating were prepared with coating's fragments: the as-received state was characterized as it was sampled; the "Dry 1st imm." sample was exposed 16 h at 60 °C before the DSC experiment; for the "Dry after 19 days of immersion" sample, some fragments of the as-received sample were immersed 19 days in a 0.5 M NaCl solution, then dried for 16 h at 60 °C before being tested. The coating fragments (around 20 mg) were sealed in standard aluminium pans. The glass transition temperature (T_g) was determined at the midpoint of the associated heat capacity jump.

3. Results

First, DSC measurements were performed to characterize the physical structure of the polyester through its glass transition temperature for the as-received sample and in the dry states. Then, from the impedance diagrams recorded for increasing immersion times in the NaCl solution, the water uptake was calculated for the three initial states of the coil coating and the modification of the impedance diagrams was discussed by taking into account the water uptake and the glass transition.

3.1. Physical structure of the coil coatings

The thermograms of the first heating ramps were obtained for the three initial states of the coil coating (the as-received and the two dry samples) and they are compared in Fig. 1.

The T_g of the as-received sample is 21 ± 1 °C whereas the T_g of the two dry samples is identical and the value is 25 ± 1 °C. For the as-received sample, an endothermic event beginning at 40 °C is associated with evaporation: it indicates the presence of water in this sample, which acts as a plasticizer. It is confirmed by the T_g value which is lower than for the dry samples ($\Delta T_g = 4$ °C). Foster et al. [32] have reported a 10 °C decrease of T_g on a polyester with a variation of relative humidity from 20 % to 80 %. Thus, the presence of water in the polymer network can reasonably be attributed to the storage conditions. Furthermore, the fact that the T_g of the dry samples are similar might indicate that the electrolyte penetration (19 days of immersion in the NaCl solution) would not induce chemical ageing of the polymer.

3.2. Electrochemical impedance results and water uptake

Fig. 2 presents some examples of the impedance spectra (Bode plots) for the as-received coil coating after 24, 168 and 456 h of immersion in a 0.5 M NaCl solution.

For the three immersion times, the curves of the impedance modulus ($|Z|$) are almost superimposed and characterized by a capacitive behaviour (straight line) indicating that the coil coating is little altered during the 456 h of immersion in the NaCl solution. The values of the impedance modulus at low frequency, higher than 10^{10} Ω cm², suggest excellent barrier properties of the coating [25,37,51,52]. In Fig. 2, it can be seen that the phase angles remain high (between 78° and 88° over the whole frequency range) in agreement with the capacitive behaviour observed for the impedance modulus. Thus, the diagrams obtained for the coil-coating are representative of an intact coating, which could be classically modelled by a simple equivalent circuit: the electrolyte

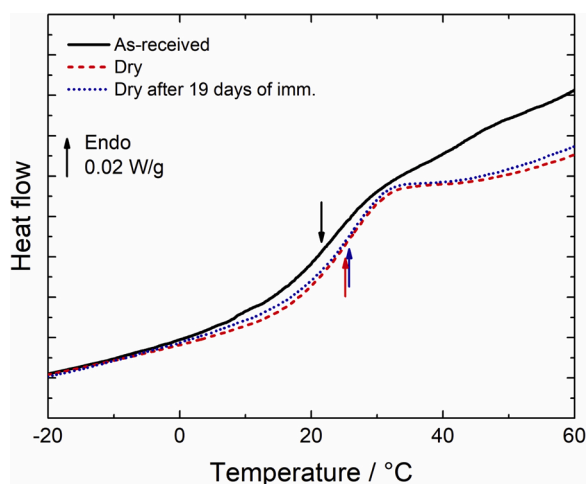


Fig. 1. DSC thermograms of the coil coating for three different initial states: as-received (continuous line), dried for 16 h at 60 °C (dashed line) and dried for 16 h at 60 °C after 19 days of immersion in a 0.5 M NaCl solution (dotted line).

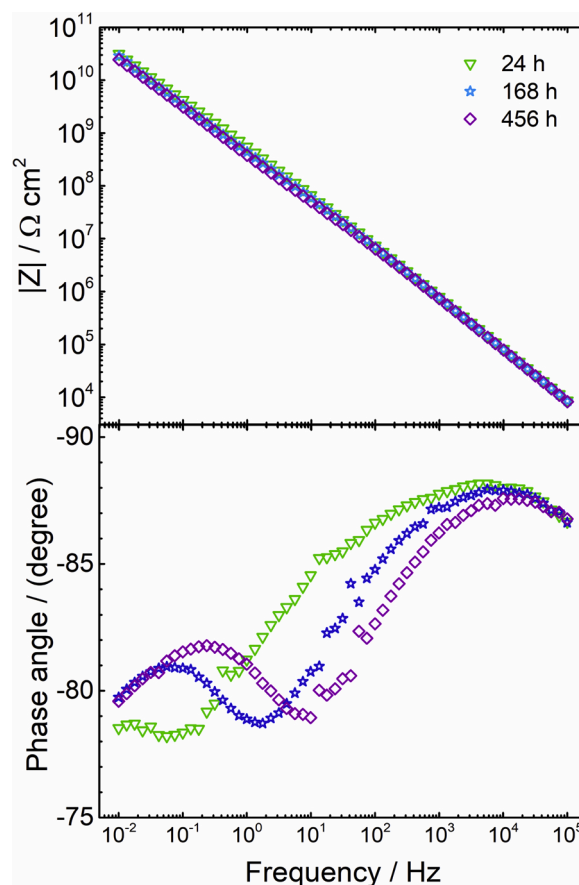


Fig. 2. EIS diagrams (Bode plots) obtained for the as-received coil coating after 24, 168 and 456 h of immersion in the 0.5 M NaCl solution.

resistance (at high frequency) in series with the coating capacitance. The coating resistance and the time constant at low frequency cannot be determined in the measurement range, whatever the immersion time. However, some changes can be noticed on the curves of the phase angle. From 6 h of immersion, a new time constant, superimposed to the phase angle decrease, can be identified. It shifts towards higher frequencies when the immersion time increases. The presence of two time constants on the impedance diagrams might be linked to the development of corrosion at the metal/coating interface but, the observed modifications can be only clearly visualised by using a magnification of the phase angle plot. This makes the hypothesis of a corrosion process unlikely. Moreover, there is no trace of blister or corrosion seen by naked eye. As already discussed in previous papers [21,39], the presence of such a time constant could represent a parameter of the coil coating material evolving through immersion time due to the water uptake. The analysis of this new time constant will be described in Section 3.3.

Then, the impedance diagrams were obtained for the dry samples during immersion in the 0.5 M NaCl solution. The diagrams obtained after 48 h and 336 h of immersion are reported in Fig. 3 and compared with those obtained for the as-received sample. The three samples present similar responses with a capacitive behaviour on the impedance modulus and the presence of the two time constants (Fig. 3a and b) which depend on the initial state of the sample. After 48 h of immersion (Fig. 3a), there is a noticeable frequency shift of the time constant, of about 1 decade between each curve. After 336 h of immersion (Fig. 3b), the three curves are quite similar, except a slight difference for the “Dry 2nd imm.” sample. This evolution will be studied in details in Section 3.3.

The water uptake was determined from the high-frequency part of the impedance data. The real part of the coating permittivity, $\epsilon'(f)$, was

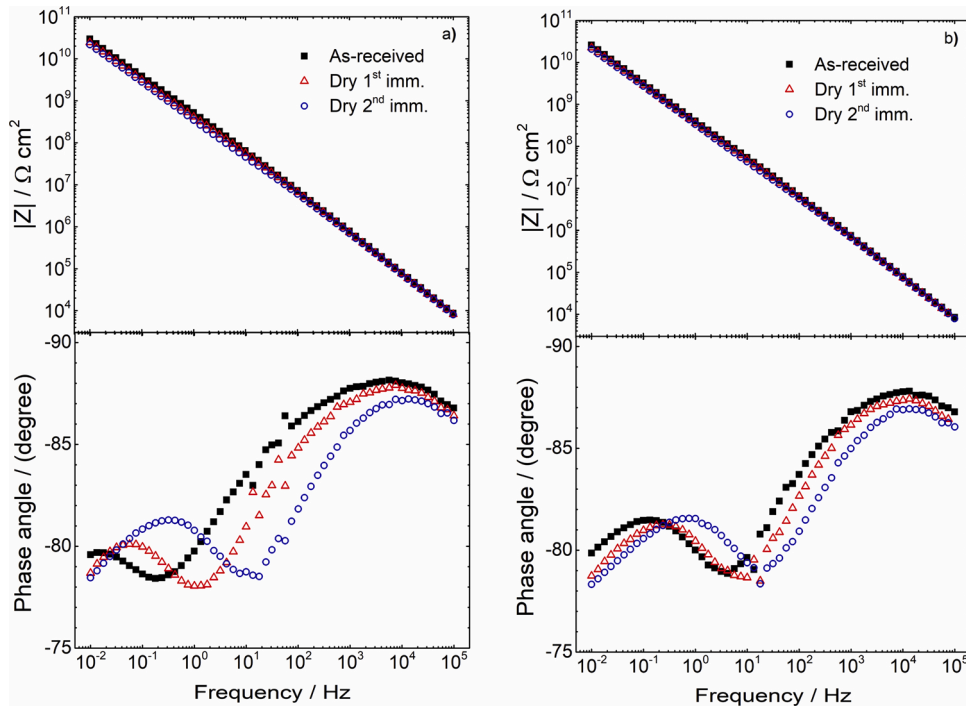


Fig. 3. EIS diagrams (Bode plots) obtained after 48 h (a) and 336 h (b) of immersion in the 0.5 M NaCl solution for the three initial states of the coil coating: as-received, dry and dry after 19 days of immersion in the 0.5 M NaCl solution.

first calculated thanks to Eqs. 1 and 2 [40].

$$\varepsilon''(f) = \frac{Z''(f)}{2\pi f C_v |Z|^2} \quad (1)$$

$$\text{With } C_v = \frac{\varepsilon_0 A}{l} \quad (2)$$

Where $Z''(f)$ is the imaginary part of the impedance at a given frequency, f , $|Z|$ is the impedance modulus, ε_0 is the vacuum permittivity, A is the surface area in contact with the electrolyte (14.6 cm²) and l the coating thickness (25 μm). The dielectric permittivity was calculated for different frequencies in the high frequency range and similar values of the water uptake were obtained. Thus, the permittivity values obtained at 60 kHz were used in the following.

Fig. 4 shows the permittivity variation as a function of the immersion time in the 0.5 M NaCl solution for the three initial states of the coil coating. In Fig. 4a, the time scale is linear. A quick increase of the permittivity can be observed during the first hours of immersion, followed by a slower increase for longer immersion times. Independently of the initial state, the coil coating permittivity does not reach a steady state value within the 456 h of the experiment. The first hour of immersion induces 26, 71 and 78 % of the total permittivity variation (during 456 h), for the as-received, the Dry 1st imm. and the Dry 2nd imm. samples, respectively. Thus, for the dry samples, the permittivity increase is mainly observed at the beginning of immersion. It can be assumed that the permittivity variation during immersion in the electrolytic solution is associated with water uptake (the permittivity of water (80 at room temperature [13]) is one order of magnitude higher than that of organic coatings). Thus, the curves of permittivity (Fig. 4a) can be analysed as water sorption curves [53]. The sorption curve for the as-received sample was fitted with a power-law as a function of the immersion time according to Eq. 3.

$$\varepsilon'(t) = \varepsilon'(t=0) + at^n \quad (3)$$

Where a is a constant (here 0.12 for the as-received sample) and n is an exponent associated with the diffusion mechanism.

The exponent n , determined for the as-received sample, is equal to 0.2. The water sorption can be qualified as “less-Fickian” [54] compared to typical Fickian diffusion ($n = 0.5$) governed by the water concentration gradient [11,12,55]. The physical mechanisms behind “less-Fickian” diffusion are not clear but has been already observed for chlorinated rubber and acrylic paints [56], and for different materials such as semi-interpenetrating polymer networks [54]. Perez et al. [56] attributed it to interactions of water molecules with the coating and not taken into account when applying the Fick’s law.

The permittivity values were plotted as a function of the immersion time to the power n (Fig. 4b) for the three initial states of the coil coating. For the as-received sample, the permittivity variation displays a linear behaviour (straight line). For the dry samples, the power-law equation (with $n = 0.2$) did not allow the experimental data to be correctly adjusted throughout the whole duration of the experiment. However, two linear parts can be obtained. For short immersion times, a fast increase (region I) and then, for longer immersion times, a slow increase of the permittivity are observed (region II). The vertical dotted line in Fig. 4b separates the two regions at about 1 h of immersion. The extrapolation to $t = 0$ of the first region ($t < 1$ h) gives the real permittivity of the sample before immersion ($\varepsilon'(t=0)$). The extrapolated permittivity values are 5.0 for the as-received sample and 4.7 for both dry samples. Thus, for the dry samples, the same initial permittivity value indicates an identical initial state.

Then, the water uptake was calculated with a linear rule of mixture (Eq. 4) taking into account the coating (polymer matrix, fillers and additives) and the adsorbed water [20–22].

$$\phi(t) = \frac{\varepsilon'(t) - \varepsilon'(t=0)}{\varepsilon'_{H_2O} - \varepsilon'(t=0)} \quad (4)$$

In Eq. 4, $\phi(t)$ is the water uptake (vol.%), $\varepsilon'(t)$ is the real part of the permittivity of the coating determined by EIS, $\varepsilon'(t=0)$ is the coating permittivity before the immersion and ε'_{H_2O} is the water permittivity at room temperature (80 [13]). The water uptake values are reported in Fig. 5.

The as-received sample displays a continuous linear increase of

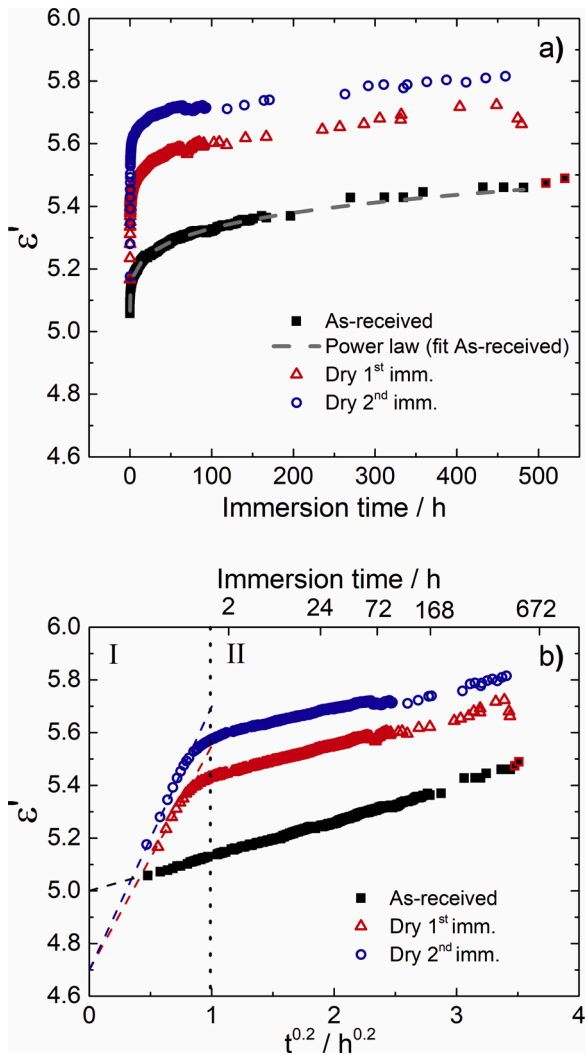


Fig. 4. Real part of the permittivity (ϵ') as a function of the immersion time in the 0.5 M NaCl solution for the three initial states of the coil coating: as-received, dry and dry after 19 days of immersion in the 0.5 M NaCl solution. (a) Immersion time with a linear scale and (b) Immersion time to the power of 0.2. The dotted line separates the two regions of the water uptake: (I) fast and (II) slow. $\epsilon'(t=0)$ are determined by linear extrapolations of the region I (dashed lines).

water uptake which reaches a value of 0.64 vol.% after 456 h of immersion. For the dry samples, two regions are observed in Fig. 5. The first one (region I) corresponds to a quick increase of the water uptake, to approximately 1.00 vol.% and 1.15 vol.% within 1 h for the 1st and 2nd immersion of the dry samples, respectively. Then, a much slower increase of the water uptake of about 0.40 vol.% for 456 h is observed (region II). Table 1 summarizes the slopes of the two water sorption kinetics observed in Fig. 5. The slopes of the region II are almost similar for the three samples but are an order of magnitude lower than those of the region I.

The presence of two water sorption kinetics for the dry samples and only one for the as-received sample can be explained through their different initial states. The absence of the region I for the as-received sample can be linked to the fact that this sample already contains water prior to the experiment due to its long-term storage (one year), in agreement with a lower T_g value (Fig. 1). Thus, region I might be associated with the filling of macroscopic porosities in the coating (less than 1 vol.%), whereas region II might correspond to a slower diffusion of water within the polymer matrix at the molecular scale. For the as-received sample, the porosities would be already filled by ambient

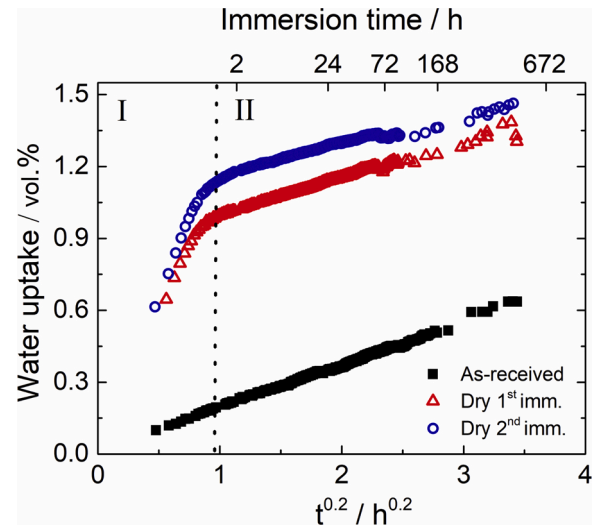


Fig. 5. Water uptake as a function of the immersion time in the 0.5 M NaCl solution for the three initial states of the coil coating: as-received, dry and dry after 19 days of immersion. The two sorption regions are separated by a dotted line.

Table 1

Slopes of the two water uptake kinetics obtained from linear fits in Fig. 5 (regions I and II).

Initial state of the coil coating	Region I (vol./h ^{0.2})	Region II (vol./h ^{0.2})
As-received	–	0.19 ± 0.01
Dry 1st imm.	1.17 ± 0.01	0.16 ± 0.01
Dry 2nd imm.	1.32 ± 0.01	0.11 ± 0.01

moisture.

The initial water content in the as-received sample is not known and therefore, Eq. 4 gives a water uptake, whereas for the initially dry samples, the water uptake is equivalent to the total water fraction. To obtain the initial permittivity value of the as-received coating (without water due to storage condition), the sample was dried after the impedance measurements and again immersed in the 0.5 M NaCl solution. Using the same protocol as for the dry samples, the $\epsilon'(t=0)$ value of the dry state was determined (results not shown) leading to a permittivity value of 4.5. From this permittivity value, the calculated water fraction in the as-received coil coating before immersion is 0.65 ± 0.15 vol.%.

After 15 days (360 h) of immersion, the amount of absorbed water for the as-received coil coating can be calculated and compared with gravimetric measurements reported in the literature. A value of 0.60 vol.% is extracted from Fig. 5 (360 h). To this value, the calculated water fraction before immersion is added (0.65 ± 0.15 vol.%) and a total water uptake of 1.25 ± 0.15 vol.% is obtained. This value is in agreement with water uptake reported in the literature on a polyester paint determined by gravimetry (1.10 vol.%) [19].

It is important to note that for the two dry samples, the water uptake is significantly different on region II (Fig. 5). This result indicates that the rate of water uptake accelerates: kinetics of region I have increased by 13 %, as seen in Table 1. This suggests that previous immersions irreversibly influenced the accessibility of water in the coating. Moreover, given the low film thickness (25 μm), the absence of a saturation plateau during the experiments is unexpected, indicating a very slow process. It might be partly responsible for the less-Fickian behaviour observed in the second region of water sorption, even at long immersion times. However, for the two dry samples, both the $\epsilon'(t=0)$ values and the T_g values were identical, meaning that no leaching and no hydrolysis occur during the 1st and the 2nd immersion [57]. This might mean that the degradation mechanism that facilitates water uptake occurs at a

different scale than the glass transition. The irreversible aspect of the water sorption kinetics may be due to a rearrangement of the polymer chains, freeing interaction sites with water. Upon re-immersion, these sites might be still available and accelerate the water ingress. On another hand, in this study, the polymer's volume was considered constant over the immersion time but swelling may occur with increasing water uptake and then may create internal stresses inside the coil coating. Cycling in wet and dry environments or extended immersion times may facilitate the accessibility to hydrophilic sites, at molecular scale [35, 41].

3.3. Time constant analysis

The time constant observed on the impedance diagrams (Figs. 2 and 3) was analysed with an approach previously described [21,39]. The impedance data were converted to the imaginary part of the permittivity thanks to Eq. 5 to emphasize dipolar phenomenon and to allow the use of mathematical tools (from the dielectric literature [40]), such as the Cole-Cole equation [58] (Eq. 6), to extract the corresponding time constant τ .

$$\varepsilon''(f) = \frac{Z'(f)}{2\pi f C_v |Z|^2} \quad (5)$$

In Eq. 5, $\varepsilon''(f)$ is the imaginary part of the permittivity, $Z'(f)$ the real part of the impedance, f is the frequency, C_v is the capacitance described in Eq. 2 and $|Z|$ is the impedance modulus of the EIS impedance. Fig. 6 presents some examples of the imaginary part of the permittivity for the as-received coil coating after 24, 168 and 456 h of immersion in a 0.5 M NaCl solution.

According to a procedure recently developed [21], EIS data were fitted with Eq. 6 to Eq. 8.

$$\varepsilon_{Cole-Cole}^*(f) = \varepsilon_\infty + \frac{\varepsilon_s - \varepsilon_\infty}{1 + (j2\pi f \tau)^\alpha} \quad (6)$$

$$\varepsilon_\sigma^*(f) = j \left(\frac{\sigma_{dc}}{2\pi f \varepsilon_0} \right)^n \quad (7)$$

$$\varepsilon^*(f) = \varepsilon_{Cole-Cole}^*(f) + \varepsilon_\sigma^*(f) \quad (8)$$

Where $\varepsilon_{Cole-Cole}^*$ corresponds to the Cole-Cole contribution [58] to the complex permittivity, ε_∞ and ε_s are the high and low frequency limits of the relative permittivity, f is the frequency, τ is the time constant, α is the exponent which describes the broadness of the peak, ε_σ^* is the conductivity contribution to the complex permittivity, σ_{dc} is the value of the

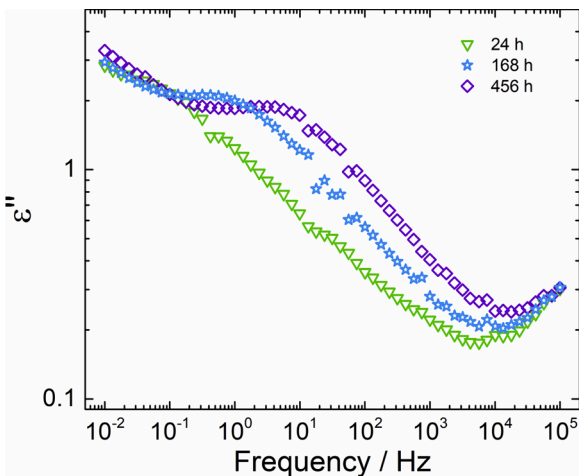


Fig. 6. Imaginary part of the dielectric permittivity (ε'') for the as-received coil coating after 24, 168 and 456 h of immersion in the 0.5 M NaCl solution.

direct current conductivity of the coil coating and n is a non-ideality exponent.

In contrast with a previous study [39], no further mathematical treatment was necessary to fit the experimental data because the conductivity contribution is sufficiently separated from the observed time constant. An example of the fit is displayed in Fig. 7.

The time constant τ was extracted from the impedance data for each immersion time in the 0.5 M NaCl solution and is reported in Fig. 8 for the three different initial states of the coil coating.

It can be seen that the time constant decreases over immersion time, going down two decades for the as-received and Dry 1st imm. coil coatings and one decade for the Dry 2nd imm. For the three initial states, the time constant does not stabilize over the 456 h of the experiment. To investigate the origin of this time constant and because we assume that water uptake is the primary process occurring in immersion, the time constant was plotted as a function of the water uptake in Fig. 9.

Fig. 9 shows that the time constants of the dry samples are nearly superimposed when represented as a function of the water uptake, which contrasts with the difference observed when plotted versus immersion time (Fig. 8). The as-received sample displays the same behaviour as the dry samples, but shifted to lower water uptake. The as-received sample already contains water at the beginning of the immersion (estimated to 0.65 ± 0.15 vol.%), which needs to be added to the water uptake to obtain the total water fraction in the coil coating. For the dry samples, the water uptake equals the total water fraction. In Fig. 10, the time constant is plotted as a function of the water volume fraction.

Fig. 10 shows that taking into account the initial water content in the as-received sample brings the time constant in the close vicinity of those of the dry samples. In Fig. 10, the error margins on the initial water content in the as-received sample allows considering the three initial states to be within the same uncertainty range. This implies that the phenomenon associated with the time constant is reversible and mostly depends on the water fraction absorbed by the coil coating.

4. Discussion

The time constant extracted from the impedance diagrams decreases over increasing water content in the coating (Fig. 10). No signs of corrosion or blistering were observed upon visual inspection of the samples. Moreover, a defective sample displaying visible corrosion signs (not shown) allowed the measurement of both a time constant associated with corrosion and the time constant studied in this paper, indicating that the two phenomena may not be linked. This suggests that the

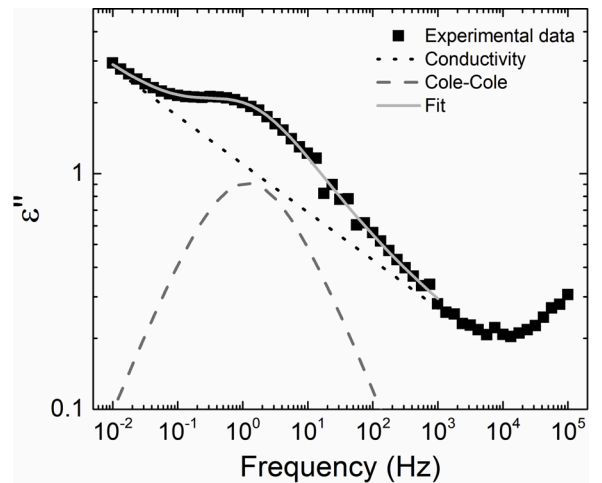


Fig. 7. Imaginary part of the dielectric permittivity (ε'') for the as-received coil coating after 168 h of immersion in the 0.5 M NaCl solution fitted with the Cole-Cole equation (Eq. 6) and a conductivity contribution (Eq. 7).

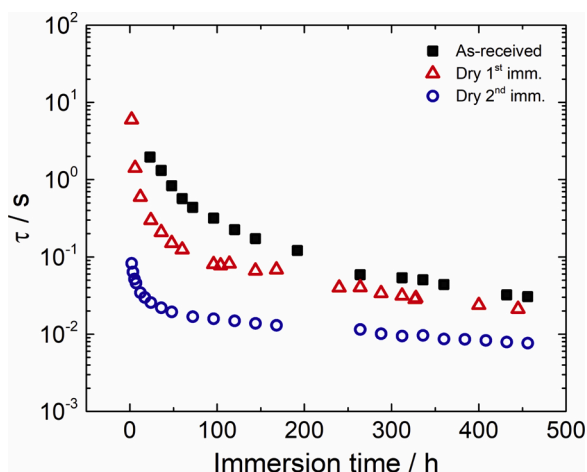


Fig. 8. Time constant (τ) as a function of immersion time in the 0.5 M NaCl solution for the three initial states of the coil coating: as-received, dry and dry after 19 days of immersion.

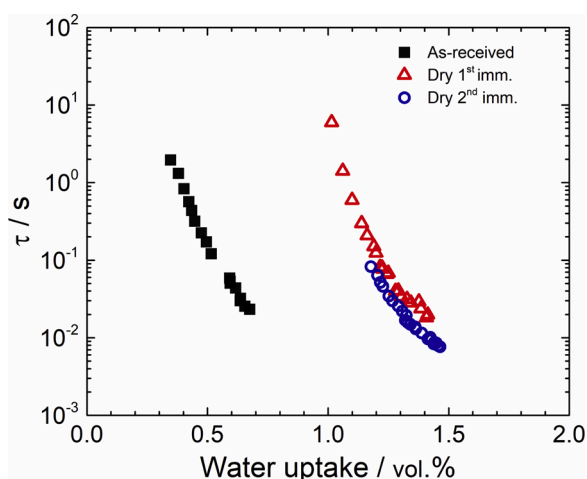


Fig. 9. Time constant (τ) as a function of water uptake for the three initial states of the coil coating: as-received, dry and dry after 19 days of immersion.

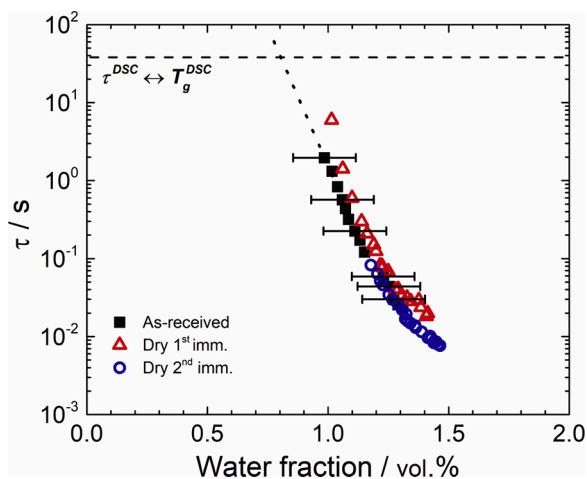


Fig. 10. Time constant (τ) as a function of water volume fraction for the three initial states of the coil coating: as-received, dry and dry after 19 days of immersion.

time constant studied here could be the dielectric manifestation of the polymer glass transition, similarly to what was recently reported for an epoxy varnish studied by thermally-controlled EIS [39]. Water being a plasticizer of the coating, it is expected that its glass transition temperature and the relaxation time of its dielectric manifestation decrease [32,40]. The time constant variations are reversible regarding the amount of plasticizer (water) incorporated within the coating. EIS is similar to the broadband dielectric spectroscopy, which probes the dipolar relaxations in polymers by applying a sinusoidal voltage over a wide range of frequencies but not in immersion. The molecular mobility modes are observed at characteristic frequencies which correspond to relaxation times, τ [59]. For the α -mode (dielectric manifestation of the glass transition), dipoles constitutive of the main polymer chain are probed, over distances of a few monomers only. The fact that τ are decreasing with increasing water fraction in the coil coating is consistent with a plasticization effect [20,45,49] and equivalent to a decrease in T_g . Unfortunately, the plasticization models based on T_g (Fox [60,61], Kelley-Bueche [62], Simha-Boyer [63]) cannot be applied to τ , and similar models for the dielectric manifestation of the glass transition do not appear to exist yet.

The T_g determined by DSC (Fig. 1) on the as-received sample (21 ± 1 °C) is close to the temperature at which the EIS experiments were made (ambient temperature). This is incidental but may be used to further correlate EIS and DSC. The heating rate during the DSC ramp (20 °C/min) indeed corresponds to a characteristic frequency (or, reciprocally, a characteristic time), as described by Hensel et al. [64]. According to the thermograms in Fig. 1, the T_g determined experimentally in the present work correspond to an equivalent characteristic time of 40 s. Under the assumption that τ is the dielectric manifestation of the glass transition in EIS, there should be a continuity between τ and T_g . A dotted line corresponding to $\tau = 40$ s is displayed in Fig. 10 and its intersection with the linear extrapolation of the EIS points (dashed line) indicates that the water content of the as-received sample is 0.80 vol.%, which is in very good agreement with the previously calculated water content (0.65 ± 0.15 vol.%) and further supports the hypothesis that the time constant is the dielectric manifestation of the glass transition. Thus, there is strong evidence that the time constant observed in EIS could be the dielectric manifestation of the glass transition of the coating. Following this time constant over time enables *in situ* observations of the effect of water uptake on the glass transition of the material. An important outcome is that the water uptake was faster after the second drying of the coating, suggesting a rearrangement of the polymer chains facilitating the water ingress.

5. Conclusions

Three different states of a commercial polyester coil-coated steel were characterized by EIS during immersion in a 0.5 M NaCl solution. First, in any case, it was shown that the impedance modulus at low frequency was high ($> 10^{10} \Omega \text{ cm}^2$) and without significant change with increasing immersion time, indicative of a good barrier effect of the coil coating.

The water sorption curves revealed two regions for the dry states of the coating: the first one corresponding to a quick increase in water content and the second region to a much slower increase. The first region observed on the dry samples was attributed to the filling of porosities, easily accessible, already saturated for the as-received sample. The second region was attributed to the diffusion of water within the polymer matrix. For the three initial states, it was shown that the coating saturation with water was not reached at the end of the test (456 h) and the analysis of the water sorption kinetics revealed a “less-Fickian” behaviour.

The time constant, τ , extracted from the impedance diagrams was linked to the water content within the coating and corresponds to the dielectric manifestation of the polymer glass transition. With increasing immersion time, τ decreased due to the plasticizing effect of water. The

knowledge of this parameter can be of great interest for the assessment of the durability of coil coatings.

It was also shown that the water uptake was faster after drying and re-immersion which also could be an important factor in the degradation of the coating. However, in the present study, blistering was not observed, even after several months of immersion. Thus, to accelerate the degradation process, the next step will be to perform impedance measurements for temperatures ranging from 40 to 60 °C.

The proposed approach allows an *in situ* analysis of both the water uptake and its effect on the physical structure of the polyester coil coating. The coating is not an inert material as it is considered in the impedance data analysis through the use of equivalent electrical circuits. This approach can be applied to study model or simplified systems and more generally to access additional data on the link between formulations and degradation mechanisms.

CRedit authorship contribution statement

Pierre Bonin: Conceptualization, Data curation, Formal analysis, Investigation, Writing - original draft. **Aurélien Roggero:** Conceptualization, Data curation, Formal analysis, Investigation, Methodology, Supervision, Writing - original draft. **Nicolas Caussé:** Conceptualization, Formal analysis, Methodology, Project administration, Supervision, Validation, Writing - review & editing. **Nadine Pèbère:** Conceptualization, Formal analysis, Methodology, Project administration, Supervision, Validation, Writing - review & editing. **Dominique Thierry:** Conceptualization, Project administration, Resources, Supervision, Validation, Writing - review & editing. **Nathalie Le Bozec:** Conceptualization, Project administration, Resources, Supervision, Validation, Writing - review & editing.

Declaration of Competing Interest

The authors declare that they have no known competing financial interests or personal relationships that could have appeared to influence the work reported in this paper.

References

- [1] T. Prosek, D. Thierry, A model for the release of chromate from organic coatings, *Prog. Org. Coat.* 49 (2004) 209–217, <https://doi.org/10.1016/j.porgcoat.2003.09.012>.
- [2] A.C. Bastos, A.M.P. Simoes, Effect of deep drawing on the performance of coil-coatings assessed by electrochemical techniques, *Prog. Org. Coat.* 65 (2009) 295–303, <https://doi.org/10.1016/j.porgcoat.2009.01.002>.
- [3] W. Funke, Blistering of paint films and filiform corrosion, *Prog. Org. Coat.* 9 (1981) 29–46, [https://doi.org/10.1016/0033-0655\(81\)80014-3](https://doi.org/10.1016/0033-0655(81)80014-3).
- [4] O. Negele, W. Funke, Internal stress and wet adhesion of organic coatings, *Prog. Org. Coat.* 28 (1996) 285–289.
- [5] F. Zou, D. Thierry, Localized electrochemical impedance spectroscopy for studying the degradation of organic coatings, *Electrochim. Acta* 42 (1997) 3293–3301, [https://doi.org/10.1016/S0013-4686\(97\)00180-1](https://doi.org/10.1016/S0013-4686(97)00180-1).
- [6] T. Prosek, A. Nazarov, J. Stouilil, D. Thierry, Evaluation of the tendency of coil-coated materials to blistering: field exposure, accelerated tests and electrochemical measurements, *Corros. Sci.* 61 (2012) 92–100, <https://doi.org/10.1016/j.corsci.2012.04.026>.
- [7] L. Fedrizzi, A. Bergo, M. Fanicchia, Evaluation of accelerated aging procedures of painted galvanised steels by EIS, *Electrochim. Acta* 51 (2006) 1864–1872, <https://doi.org/10.1016/j.electacta.2005.02.146>.
- [8] F. Deflorian, L. Fedrizzi, Adhesion characterization of protective organic coatings by electrochemical impedance spectroscopy, *J. Adhes. Sci. Technol.* 13 (1999) 629–645, <https://doi.org/10.1163/156856199X00154>.
- [9] M. Ohman, D. Persson, An integrated *in situ* ATR-FTIR and EIS set-up to study buried metal-polymer interfaces exposed to an electrolyte solution, *Electrochim. Acta* 52 (2007) 5159–5171, <https://doi.org/10.1016/j.electacta.2007.02.007>.
- [10] P. Taheri, H. Terry, J.M.C. Mol, Studying interfacial bonding at buried polymer-mercuric interfaces, *Prog. Org. Coat.* 89 (2015) 323–331, <https://doi.org/10.1016/j.porgcoat.2015.03.017>.
- [11] E.P.M. van Westing, G.M. Ferrari, J.H.W. de Wit, The determination of coating performance with impedance measurements-II. Water uptake of coatings, *Corros. Sci.* 36 (1994) 957–977, [https://doi.org/10.1016/0010-938X\(94\)90197-X](https://doi.org/10.1016/0010-938X(94)90197-X).
- [12] T. Naylor, Permeation properties, in: G. Allen, J.C. Bevington (Eds.), *Compr. Polym. Sci. Suppl.*, Pergamon, 1989, pp. 643–668, <https://doi.org/10.1016/b978-0-08-096701-1.00057-4>.
- [13] D.M.M. Brasher, A.H.H. Kingsbury, Electrical measurements in the study of immersed paint coatings on metal. 1. Comparison between capacitance and gravimetric methods of estimating water-uptake, *J. Appl. Chem.* 4 (1954) 62–72, <https://doi.org/10.1002/jctb.5010040202>.
- [14] A.S. Castela, A.M. Simoes, Water sorption in freestanding PVC films by capacitance measurements, *Prog. Org. Coat.* 46 (2003) 130–134, [https://doi.org/10.1016/S0300-9440\(02\)00220-5](https://doi.org/10.1016/S0300-9440(02)00220-5).
- [15] M. Kendig, J. Scully, Basic aspects of electrochemical impedance application for the life prediction of organic coatings on metals, *Corrosion.* 46 (1990) 22–29, <https://doi.org/10.5006/1.3585061>.
- [16] L. Philippe, C. Sammon, S.B. Lyon, J. Yarwood, An FTIR/ATR *in situ* study of sorption and transport in corrosion protective organic coatings 1. Water sorption and the role of inhibitor anions, *Prog. Org. Coat.* 49 (2004) 302–314, <https://doi.org/10.1016/j.porgcoat.2003.07.002>.
- [17] M. Ohman, D. Persson, C. Leygraf, *In situ* ATR-FTIR studies of the aluminium/polymer interface upon exposure to water and electrolyte, *Prog. Org. Coat.* 57 (2006) 78–88, <https://doi.org/10.1016/j.porgcoat.2006.07.002>.
- [18] C. Vosgien Lacombe, G. Bouvet, D. Trinh, S. Mallarino, S. Touzain, Water uptake in free films and coatings using the Brasher and Kingsbury equation: a possible explanation of the different values obtained by electrochemical impedance spectroscopy and gravimetry, *Electrochim. Acta* 231 (2017) 162–170, <https://doi.org/10.1016/j.electacta.2017.02.051>.
- [19] A.S. Castela, A.M. Simoes, Assessment of water uptake in coil coatings by capacitance measurements, *Prog. Org. Coat.* 46 (2003) 55–61, [https://doi.org/10.1016/S0300-9440\(02\)00190-X](https://doi.org/10.1016/S0300-9440(02)00190-X).
- [20] A.S. Nguyen, N. Causse, M. Musiani, M.E. Orazem, N. Pèbère, B. Tribollet, V. Vivier, Determination of water uptake in organic coatings deposited on 2024 aluminium alloy: comparison between impedance measurements and gravimetry, *Prog. Org. Coat.* 112 (2017) 93–100, <https://doi.org/10.1016/j.porgcoat.2017.07.004>.
- [21] A. Roggero, L. Villareal, N. Caussé, A. Santos, N. Pèbère, Correlation between the physical structure of a commercially formulated epoxy paint and its electrochemical impedance response, *Prog. Org. Coat.* 146 (2020), 105729, <https://doi.org/10.1016/j.porgcoat.2020.105729>.
- [22] A.S. Castela, A.M. Simoes, An impedance model for the estimation of water absorption in organic coatings. Part I: a linear dielectric mixture equation, *Corros. Sci.* 45 (2003) 1631–1646, [https://doi.org/10.1016/S0010-938X\(03\)00014-3](https://doi.org/10.1016/S0010-938X(03)00014-3).
- [23] G.K. Van Der Wel, O.C.G. Adan, Moisture in organic coatings - a review, *Prog. Org. Coat.* 37 (1999) 1–14, [https://doi.org/10.1016/S0300-9440\(99\)00058-2](https://doi.org/10.1016/S0300-9440(99)00058-2).
- [24] A. Cao-Paz, A. Covelo, J. Farina, X.R. Nóvoa, C. Pérez, L. Rodríguez-Pardo, Ingress of water into organic coatings: real-time monitoring of the capacitance and increase in mass, *Prog. Org. Coat.* 69 (2010) 150–157, <https://doi.org/10.1016/j.porgcoat.2010.04.004>.
- [25] J.E.O. Mayne, The mechanism of the inhibition of the corrosion of iron and steel by means of paint, *Anti Corros. Methods Mater.* 20 (1974) 286–290.
- [26] L. Fedrizzi, F. Deflorian, G. Boni, P.L. Bonora, E. Pasini, EIS study of environmentally friendly coil coating performances, *Prog. Org. Coat.* 29 (1996) 89–96, [https://doi.org/10.1016/S0300-9440\(96\)00620-0](https://doi.org/10.1016/S0300-9440(96)00620-0).
- [27] F. Mansfeld, M.W. Kendig, S. Tsai, Evaluation of corrosion behavior of coated metals with AC impedance measurements, *Corrosion* 38 (1982) 478–485, <https://doi.org/10.5006/1.3577363>.
- [28] V.B. Miskovic-Stankovic, D.M. Dražić, Z. Kačarević-Popović, The sorption characteristics of epoxy coatings electrodeposited on steel during exposure to different corrosive agents, *Corros. Sci.* 38 (1996) 1513–1523, [https://doi.org/10.1016/0010-938X\(96\)00042-X](https://doi.org/10.1016/0010-938X(96)00042-X).
- [29] M.M. Wind, H.J.W. Lenderink, A capacitance study of pseudo-fickian diffusion in glassy polymer coatings, *Prog. Org. Coat.* 28 (1996) 239–250, [https://doi.org/10.1016/0300-9440\(95\)00601-X](https://doi.org/10.1016/0300-9440(95)00601-X).
- [30] N. Coniglio, K. Nguyen, R. Kurji, E. Gamboa, Characterizing water sorption in 100 % solids epoxy coatings, *Prog. Org. Coat.* 76 (2013) 1168–1177, <https://doi.org/10.1016/j.porgcoat.2013.03.011>.
- [31] T.S. Ellis, F.E. Karasz, Interaction of epoxy resins with water: the depression of glass transition temperature, *Polymer (Guildf)* 25 (1984) 664–669, [https://doi.org/10.1016/0032-3861\(84\)90034-X](https://doi.org/10.1016/0032-3861(84)90034-X).
- [32] G.M. Foster, S. Ritchie, K.E. Evans, C. Lowe, Controlled relative humidity testing for the characterisation of the brittle-tough and glass transition temperatures of coil coating paint films, *Prog. Org. Coat.* 51 (2004) 244–249, <https://doi.org/10.1016/j.porgcoat.2004.08.002>.
- [33] J.T. Zhang, J.M. Hu, J.Q. Zhang, C.N. Cao, Studies of water transport behavior and impedance models of epoxy-coated metals in NaCl solution by EIS, *Prog. Org. Coat.* 51 (2004) 145–151, <https://doi.org/10.1016/j.porgcoat.2004.08.001>.
- [34] L.S. Nacher, J.E.C. Amoros, M.D.S. Moya, J.L. Martínez, Mechanical properties of polyester resins in saline water environments, *Int. J. Polym. Anal. Charact.* 12 (2007) 373–390, <https://doi.org/10.1080/10236660701516557>.
- [35] S.G. Croll, Electrolyte transport in polymer barrier coatings: perspectives from other disciplines, *Prog. Org. Coat.* 124 (2018) 41–48, <https://doi.org/10.1016/j.porgcoat.2018.07.027>.
- [36] G. Lendvay-Gyorik, T. Pajkossy, B. Lengyel, Corrosion-protection properties of water-borne paint coatings as studied by electrochemical impedance spectroscopy and gravimetry, *Prog. Org. Coat.* 56 (2006) 304–310, <https://doi.org/10.1016/j.porgcoat.2006.05.012>.
- [37] G.P. Bierwagen, L. He, J. Li, L. Ellingson, D.E. Tallman, Studies of a new accelerated evaluation method for coating corrosion resistance - thermal cycling testing, *Prog. Org. Coat.* 39 (2000) 67–78, [https://doi.org/10.1016/S0300-9440\(00\)00106-5](https://doi.org/10.1016/S0300-9440(00)00106-5).

- [38] L. Valentinelli, J. Vogelsang, H. Ochs, L. Fedrizzi, Evaluation of barrier coatings by cycling testing, *Prog. Org. Coat.* 45 (2002) 405–413, [https://doi.org/10.1016/S0300-9440\(02\)00137-6](https://doi.org/10.1016/S0300-9440(02)00137-6).
- [39] A. Roggero, N. Caussé, E. Dantras, L. Villareal, A. Santos, N. Pèbère, Thermal activation of impedance measurements on an epoxy coating for the corrosion protection: 2. electrochemical impedance spectroscopy study, *Electrochim. Acta* 305 (2019) 116–124, <https://doi.org/10.1016/j.electacta.2019.03.007>.
- [40] F. Kremer, A. Schonhals, *Broadband Dielectric Spectroscopy*, Springer Science & Business Media, 2002.
- [41] N.A. Brunt, Blistering of paint layers as an effect of swelling by water, *J. Oil Colour Chem. Assoc.* 47 (1964) 31–42.
- [42] C. Vosgien Lacombe, G. Bouvet, D. Trinh, S. Mallarino, S. Touzain, Effect of pigment and temperature onto swelling and water uptake during organic coating ageing, *Prog. Org. Coat.* 124 (2018) 249–255, <https://doi.org/10.1016/j.porgcoat.2017.11.022>.
- [43] S. Shreepathi, S.M. Naik, M.R. Vattipalli, Water transportation through organic coatings: correlation between electrochemical impedance measurements, gravimetry, and water vapor permeability, *J. Coatings Technol. Res.* 9 (2012) 411–422, <https://doi.org/10.1007/s11998-011-9376-4>.
- [44] R.M. Souto, Y. González-García, S. González, G.T. Burstein, Imaging the origins of coating degradation and blistering caused by electrolyte immersion assisted by SECM, *Electroanalysis* 21 (2009) 2569–2574, <https://doi.org/10.1002/elan.200900262>.
- [45] G. Grundmeier, W. Schmidt, M. Stratmann, Corrosion protection by organic coatings: electrochemical mechanism and novel methods of investigation, *Electrochim. Acta* 45 (2000) 2515–2533, [https://doi.org/10.1016/S0013-4686\(00\)00348-0](https://doi.org/10.1016/S0013-4686(00)00348-0).
- [46] I.C.P. Margarit-Mattos, EIS and organic coatings performance: revisiting some key points, *Electrochim. Acta* 354 (2020), 136725, <https://doi.org/10.1016/j.electacta.2020.136725>.
- [47] A. Amirudin, D. Thierry, Application of electrochemical impedance spectroscopy to study the degradation of polymer-coated metals, *Prog. Org. Coat.* 26 (1995) 1–28, [https://doi.org/10.1016/0300-9440\(95\)00581-1](https://doi.org/10.1016/0300-9440(95)00581-1).
- [48] F. Mansfeld, C.H. Tsail, Determination of coating deterioration with EIS. I. Basic relationships, *Corrosion* 47 (1991) 958–963, <https://doi.org/10.5006/1.3585209>.
- [49] G. Bouvet, D.D. Nguyen, S. Mallarino, S. Touzain, Analysis of the non-ideal capacitive behaviour for high impedance organic coatings, *Prog. Org. Coat.* 77 (2014) 2045–2053, <https://doi.org/10.1016/j.porgcoat.2014.02.008>.
- [50] D. Loveday, P. Peterson, B. Rodgers, Evaluation of organic coatings with electrochemical impedance spectroscopy part 2: application of EIS to coatings, *JCT CoatingsTech.* 1 (2004) 88–93.
- [51] C.G. Oliveira, M.G.S. Ferreira, Ranking high-quality paint systems using EIS. Part I: intact coatings, *Corros. Sci.* 45 (2003) 123–138, [https://doi.org/10.1016/S0010-938X\(02\)00088-4](https://doi.org/10.1016/S0010-938X(02)00088-4).
- [52] M. Kendig, D.J. Mills, An historical perspective on the corrosion protection by paints, *Prog. Org. Coat.* 102 (2017) 53–59, <https://doi.org/10.1016/j.porgcoat.2016.04.044>.
- [53] A. Roggero, N. Caussé, E. Dantras, L. Villareal, A. Santos, N. Pèbère, In situ study of the temperature activated kinetics of water sorption in an epoxy varnish, *Polymer* 213 (2021), 123206, <https://doi.org/10.1016/j.polymer.2020.123206>.
- [54] A.K. Bajpai, J. Bajpai, S. Shukla, Water sorption through a semi-interpenetrating polymer network (IPN) with hydrophilic and hydrophobic chains, *React. Funct. Polym.* 50 (2002) 9–21, [https://doi.org/10.1016/S1381-5148\(01\)00085-2](https://doi.org/10.1016/S1381-5148(01)00085-2).
- [55] F. Bellucci, L. Nicodemo, Water transport in organic coatings, *Corrosion* 49 (1993) 235–247, <https://doi.org/10.5006/1.3316044>.
- [56] C. Pérez, A. Collazo, M. Izquierdo, P. Merino, X.R. Nóvoa, Characterisation of the barrier properties of different paint systems. Part II. Non-ideal diffusion and water uptake kinetics, *Prog. Org. Coat.* (1999), [https://doi.org/10.1016/S0300-9440\(99\)00073-9](https://doi.org/10.1016/S0300-9440(99)00073-9).
- [57] P.A. Sørensen, S. Kiil, K. Dam-Johansen, C.E. Weinell, Anticorrosive coatings: a review, *J. Coatings Technol. Res.* 6 (2009) 135–176, <https://doi.org/10.1007/s11998-008-9144-2>.
- [58] K.S. Cole, R.H. Cole, Dispersion and absorption in dielectrics I. Alternating current characteristics, *J. Chem. Phys.* 9 (1941) 341–351, <https://doi.org/10.1063/1.1750906>.
- [59] J.L. Halary, F. Lauprêtre, *De la macromolécule au matériau polymère*, Belin, 2006.
- [60] P.C. Hiemenz, T.P. Lodge, 12. Glass transition. *Polym. Chem, 2nd ed.*, CRC Press, Boca Raton, FL, 2007, pp. 465–509.
- [61] T.G. Fox, P.J. Flory, Second-order transition temperatures and related properties of polystyrene. I. Influence of molecular weight, *J. Appl. Phys.* 21 (1950) 581–591, <https://doi.org/10.1063/1.1699711>.
- [62] F.N. Kelley, F. Bueche, Viscosity and glass temperature relations for polymer-diluent systems, *J. Polym. Sci.* 50 (1961) 549–556, <https://doi.org/10.1002/pol.1961.1205015421>.
- [63] R. Simha, R.F. Boyer, On a general relation involving the glass temperature and coefficients of expansion of polymers, *J. Chem. Phys.* 37 (1962) 1003–1007, <https://doi.org/10.1063/1.1733201>.
- [64] A. Hensel, J. Dobberty, J.E.K. Schawe, A. Boller, C. Schick, Dielectric spectroscopy and calorimetry in the glass transition region of polymers, *J. Therm. Anal.* 46 (1996) 935–954, <https://doi.org/10.1007/BF01983612>.